

Tailoring Spectral Sensors for Specific Applications

*D.M.J. van Elst¹, A. van Klinken¹, F. Ou^{1,2}, M.S. Cano-Velázquez¹, C. Li¹,
M. Petruzzella^{1,2}, P.J. van Veldhoven¹ and A. Fiore¹*

¹ Department of Applied Physics and Science Education, Eindhoven Hendrik Casimir Institute, Eindhoven University of Technology, PO Box 513, NL 5600 MB Eindhoven, The Netherlands.

² MantiSpectra B.V., High Tech Campus 9, 5656 AE Eindhoven, The Netherlands.

Corresponding author: d.m.j.v.elst@tue.nl

Summary:

Spectral sensing in the near-infrared is a powerful method for non-destructive analysis of material composition in a wide variety of applications. A spectral sensor typically consists of an array of detectors, each responsive in a given spectral band. We have demonstrated an algorithm capable of tailoring spectral sensors to specific applications. By optimizing for all combinations of spectral bands a non-trivial solution can be found, outperforming hand-picked designs. High sensing performance can be achieved even with a few pixels, resulting in cost-effective spectral sensors with simple read-out.

Keywords: “Spectral sensors”, “application-specific”, “optimization”, “near-infrared”, “noise”

Motivation

Spectral sensing using near-infrared (NIR) light is becoming increasingly valuable for material analysis. The NIR region contains overtones of molecular bonds, enabling the analysis of chemical composition in a wide variety of fields. For this reason, miniaturized, portable sensing solutions are sought to replace expensive and bulky lab equipment in the chemical and agricultural sectors. We have earlier demonstrated a 16-pixel array of resonant-cavity detectors (900-1700nm) with a footprint of 2.25mm², without movable parts, providing robust performance for on-field sensing [1]. Fabrication can be done using optical lithography, making it suitable for mass production [2]. This method has proven effective for a wide variety of applications [3].

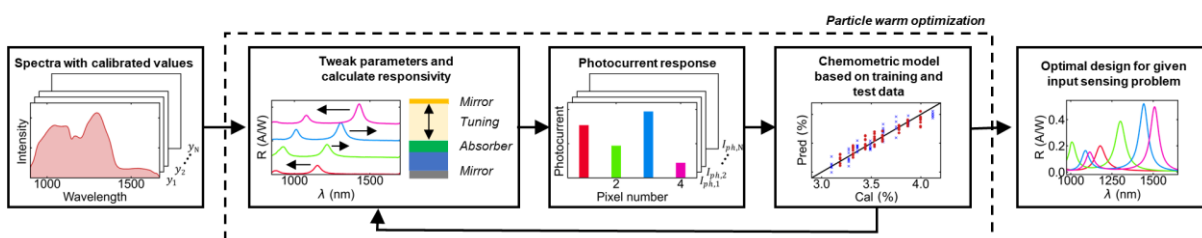
Due to the broad and overlapping spectral signatures of chemical bonds in solids and liquids, there is a lot of redundant information in NIR spectra. For example in filter-based sensing approaches this results in efforts to tailor the

filter responses to suit the applications [4-7]. We propose and demonstrate an approach to the optimization of the number and structure of the pixels in a NIR spectral sensor to achieve improved performance and reduced fabrication and read-out complexity.

The effectiveness of such an approach is demonstrated for the measurement of ethanol concentration in water. We show that, even with a few pixels, high sensing performance can be achieved. Using a numerical optimization algorithm can result in a non-trivial solution that outperforms handpicked designs. Especially in noisy environments, fewer pixels on the same sensing area can outperform a higher number of channels due to increased signal-to-noise ratio (SNR), which is valuable in sensing systems with low optical throughput.

Method

The application-specific optimization is schematically represented in Fig.1. Our sensor pixels consist of InGaAs photodiodes integrated with a Fabry-Perot cavity, where the thickness



DOI: 10.5162/EUROSENSORSXXXVI/OT7.43

of a tuning layer controls the spectral position of the responsivity peaks. We note that each pixel presents multiple peaks, which makes intuition-based optimization challenging. In order to predict the performance of a sensor array with arbitrary configuration, the responsivity curves are simulated using the transfer-matrix method. The photocurrents are simulated by integrating the incident spectrum with the responsivity curves of each pixel. By applying white noise with standard deviation σ to the photocurrents, the result can be scaled to SNR. The photocurrents can be used for partial least squares (PLS) modelling to obtain the prediction accuracy of this configuration for the sensing problem. The accuracy is optimized using a particle-swarm optimization (PSO), where the input parameters are the thicknesses of the tuning layers which determines the resonant wavelengths. When varying the number of pixels the sensing area is kept the same, meaning that a 1-pixel device is expected to have 16 times the signal of a 16-pixel sensor. Additionally, the performance of an array is averaged over a range of noise values, corresponding to the experimental situation. In the optimization 60% of the dataset is used and 40% is kept as test data for the final design.

Results

Fig. 2 shows the results of the optimization applied to a dataset of transmission spectra for mixtures of ethanol in water, with varying concentrations from 0% to 53%. The optimization is performed for varying pixel configurations. It can be seen that the root-mean-square error of the PLS prediction increases with increasing noise σ for all amounts of pixels. Most notably, there are noise regions where a 4-pixel device outperforms 8- and 16-pixel devices.

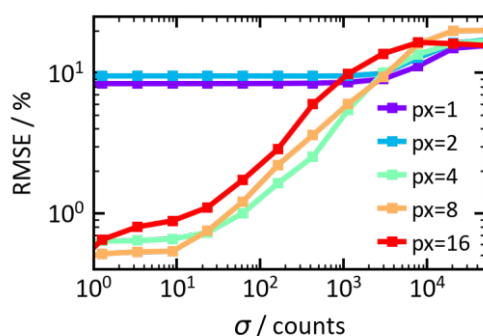


Fig. 1. Error of prediction vs noise on the readout for arrays with varying amounts of pixels.

Since this region corresponds to the expected SNR of our sensor, a 4-pixel device was further investigated before fabrication. Fig 3a shows the improving ratio of performance to deviation (RPD) on the training data throughout the iterations of the PSO. Because there are a lot of

initial evaluations, the starting point is already reasonably good. An evaluation on test data kept outside of the optimization with $\sigma=1$, the optimal case in our region of interest, shows potential for up to RPD=22.1 (Fig. 3b). As an RPD of around 3-4 is generally considered a good model, this shows that even with few pixels, high sensing performance can be achieved. As a lower number of pixels reduces the complexity of fabrication and packaging, these results show the potential of application-specific spectral sensing. An experimental demonstration of this concept is under way and will be discussed at the conference.

This research was partially funded by the Nederlandse Organisatie voor Wetenschappelijk Onderzoek (NWO) Toegepaste en Technische Wetenschappen (TTW) project n. 17626 & 16670 and the NWO Nationale Wetenschapsagenda (NWA) Kleine Projecten NWA.1418.22.022.

References

- [1] Hakkel, K. D., Petruzzella, M., Ou, F., Liu, T., Pagliano, F., Veldhoven, R. P. J. Van, & Fiore, A. Integrated near-infrared spectral sensing. *Nature Communications* 13, (2022); doi: [10.1038/s41467-021-27662-1](https://doi.org/10.1038/s41467-021-27662-1)
- [2] Klinken, A. van, Elst, D. M. J. van, Li, C., Petruzzella, M., Hakkel, K. D., Ou, F., Pagliano, F., Veldhoven, R. van, & Fiore, A. High-performance photodetector arrays for near-infrared spectral sensing. *APL Photonics* 8, (2023); doi: [10.1063/5.0136921](https://doi.org/10.1063/5.0136921)
- [3] Ou, F., van Klinken, A., Ševo, P., Petruzzella, M., Li, C., van Elst, D. M. J., Hakkel, K. D., Pagliano, F., van Veldhoven, R. P. J., & Fiore, A. Handheld NIR Spectral Sensor Module Based on a Fully-Integrated Detector Array. *Sensors* 22 (2022); doi: [10.3390/S22187027](https://doi.org/10.3390/S22187027)
- [4] Nelson, M. P., Aust, J. F., Dobrowolski, J. A., Verly, P. G., & Myrick, M. L. Multivariate Optical Computation for Predictive Spectroscopy. *Analytical Chemistry* 70 (1998); doi: [10.1021/AC970791W/ASSET/IMAGES/LARGE/AC970791WF00015.JPEG](https://doi.org/10.1021/AC970791W/ASSET/IMAGES/LARGE/AC970791WF00015.JPEG)
- [5] Tan, H., Cadusch, J. J., Meng, J., & Crozier, K. B., Genetic optimization of mid-infrared filters for a machine learning chemical classifier. *Optics Express* 30(11), 18330–18347 (2022); doi: [10.1364/OE.459067](https://doi.org/10.1364/OE.459067)
- [6] J. Waterhouse, D., & Stoyanov, D., Optimized spectral filter design enables more accurate estimation of oxygen saturation in spectral imaging. *Biomedical Optics Express* 13, 2156. (2022); doi: [10.1364/boe.446975](https://doi.org/10.1364/boe.446975)
- [7] Ayala, L., Isensee, F., Wirkert, S. J., Vemuri, A. S., Maier-Hein, K. H., Fei, B., & Maier-Hein, L., Band selection for oxygenation estimation with multispectral/hyperspectral imaging. *Biomedical Optics Express* 13, 1224-1242, 13(3), 1224–1242 (2022); doi: [10.1364/BOE.441214](https://doi.org/10.1364/BOE.441214)